

## Preparation of Retarders with a Tilted Optic Axis

Peter VAN DE WITTE\*, Jos van HAAREN, Jos TUIJTELAARS, Sjoerd STALLINGA and Johan LUB

Philips Research Laboratories, Professor Holstlaan 4, 5656 AA, Eindhoven, The Netherlands

(Received September 2, 1998; accepted for publication November 11, 1998)

Foils with a tilted optic axis can be used as compensation foils for active matrix twisted nematic displays. A method is described for preparing these foils. The method makes use of the differences in alignment for liquid crystals at the liquid crystal-air interface and the liquid crystal-substrate interface. The retardation as a function of the angle of incidence was used to analyze the director profile. Layers with tilt angles close to  $0^\circ$  were obtained from a low molecular weight glass-forming liquid crystal and a side-chain liquid crystalline polymer. Layers with high average tilt angles could be obtained by photopolymerizing thin layers of cyanobiphenyl derivatives and a liquid crystalline diacrylate. The tilt angle of the liquid crystal at the liquid crystal-air interface could be varied between  $90^\circ$  in the case of mixtures with high contents of cyanobiphenyl derivatives and to  $20^\circ$  in the case of mixtures with high contents of diacrylates.

KEYWORDS: Viewing angle, retarders, tilted optic axis, liquid crystalline polymers, reactive liquid crystals

### 1. Introduction

In liquid crystal displays various types of birefringent foils (retarders) are used (Fig. 1). Retarders that find most widespread applications are wave plates. For example, retarders with retardations ranging from 100–2000 nm can be used to influence the wavelength dependence of the transmission of supertwisted nematic (STN) displays.<sup>1)</sup> For STN displays more advanced retarders are also useful. Biaxial retarders with  $n_x > n_z > n_y$  can be used to improve the angular dependence of brightness of STN displays.<sup>2,3)</sup> Retarders with a twisted director profile can be used to replace the bulky passive cell normally used in double cell supertwisted nematic displays.<sup>4–6)</sup>

In the case of active matrix twisted nematic displays the angular dependence of the contrast values can be improved by introducing foils with birefringent properties complementary to the birefringent properties of the liquid crystals in the display in the addressed state. Because of the complex director profile, foils with a tilted optic axis have to be used. Fuji demonstrated the effectiveness of negatively birefringent foils with a tilted optic axis.<sup>7)</sup> An effective negative birefringence can also be obtained by combining two positively birefringent foils. Recently, we described the use of positively birefringent foils with a tilted optic axis in active matrix compensators.<sup>8,9)</sup>

The conventional uniaxial or biaxial retarders are usually prepared through uniaxial or biaxial stretching of polymer films (for example, polycarbonate or polyvinylalcohol). Liquid crystalline monomers and polymers can also be used for the preparation of birefringent foils.<sup>10,11)</sup> The orientation of liquid crystals can be easily manipulated to obtain conventional waveplates or more complex structures like twisted retarders. In this paper, a method for the preparation of positively birefringent retarders with a tilted optic axis will be explored. The method makes use of the differences in alignment for liquid crystals at the liquid crystal-air interface and the liquid crystal-substrate interface. Several classes of liquid crystalline materials were used for the preparation of birefringent layers. Photopolymerizable liquid crystals, a nematic side chain liquid crystalline polymer and a glass-forming low molar mass liquid crystal were investigated as materials for

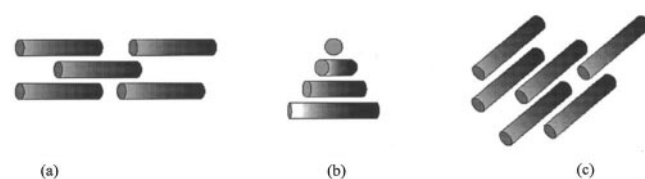


Fig. 1. Some examples of retardation foils that can be used in liquid crystal displays. (a) uniaxial non-tilted retarder, (b) twisted retarder, (c) retarder with a tilted optic axis.

retarders. The differences found in the tilt angles will be related to the chemical structures of the compounds.

### 2. Experimental

#### 2.1 Materials

The structural formulas of the compounds are shown in Fig. 2. K21 was obtained from Merck Ltd. (Poole, GB). CB6 was made according to procedures described elsewhere.<sup>12)</sup> C6Ph was made in a similar way as its hydrogen analogue, by replacing hydroquinone by 2,5-dihydroxybiphenyl.<sup>13)</sup> PolyCN was made as described before.<sup>14)</sup> The synthesis of TetraCN will be published elsewhere.<sup>15)</sup> The solvents chlorobenzene and THF (spectroscopic quality) were obtained from E. Merck (Germany). The photoinitiator Irgacure 651 was obtained from Ciba Geigy (Switzerland).

#### 2.2 Methods

Glass plates were provided with a polyimide alignment layer (AL1051, JSR, Japan). The polyimide layers were gently rubbed with a velvet cloth. Next, the liquid crystals were dissolved in chlorobenzene and spincoated on the polyimide layers. The concentration of Irgacure 651 in the mixtures of reactive liquid crystals was 1%. After spincoating the samples were kept in a nitrogen atmosphere at room temperature for several minutes and subsequently photopolymerized (Philips PL10 UV lamp,  $0.8 \text{ mW/cm}^2$ ).

The refractive indices of the layers and the pretilt of the liquid crystals on the polyimide were measured in antiparallel assembled cells. The refractive indices of the foils were determined using an Abbe refractometer ( $n_D^{25}$ ).

The photopolymerization of the mixtures of reactive liquid crystals was investigated using a DSC (Perkin Elmer DSC7) equipped with a UV light source (Philips PL10,  $0.7 \text{ mW/cm}^2$ ).

\*E-mail address: witte@natlab.research.philips.com

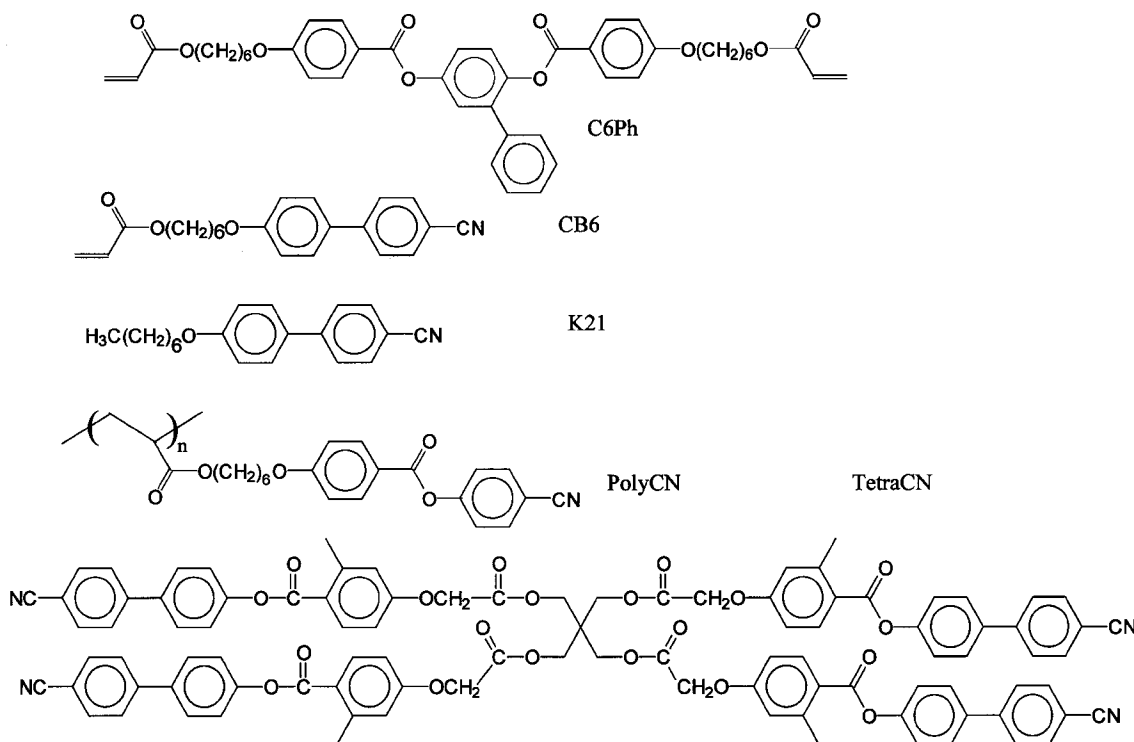
Van de Witte *et al.*: Preparation of Retarders with a Tilted Optic Axis

Fig. 2. Structural formulas of the compounds.

Molecular weights were determined using GPC relative to polystyrene standards.

The phase transition temperatures were determined using a polarization microscope provided with a hot stage (heating rate  $1^\circ\text{C}/\text{min}$ ).

The retardation of the foils as a function of the angle of incidence were measured using ellipsometer equipment described in refs. 16 and 17. Thicknesses were determined using a Dektak profilometer. The thickness of the samples was kept at approximately  $0.6\ \mu\text{m}$ . The conoscopic images were obtained using Eldim EZ Contrast 160D equipment (Caen, France).

### 3. Results

#### 3.1 Materials

The phase transitions of the compounds are indicated in Table I.

After spincoating, the mixtures should remain liquid crystalline at room temperature. The reactive liquid crystals used in this study were all nematic at room temperature. The rate of crystallization of the mixtures was sufficiently low to allow the liquid crystals to be processed at room temperature in this nematic phase. The nematic-to-isotropic phase transition

Table I. Phase transition temperatures of the compounds.

	$T_m(^{\circ}\text{C})$	$T_{N-I}(^{\circ}\text{C})$	$T_g(^{\circ}\text{C})$
K21	31	43	—
CB6	73	44	—
C6Ph	56	43	—
PolyCN	—	102	23
TetraCN	127	225	78

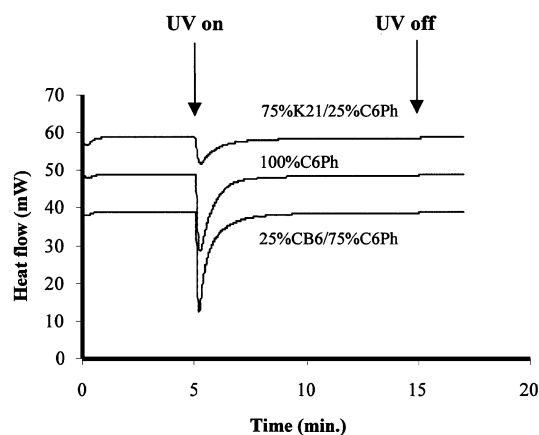


Fig. 3. DSC trace of the room temperature photopolymerization of several mixtures.

temperatures of the mixtures of K21/C6Ph and CB6/C6Ph were virtually not dependent on the composition and were approximately  $43^\circ\text{C}$ . The molecular weight ( $M_n$ ) and polydispersity ( $M_w/M_n$ ) of polyCN were  $6000\ \text{g}/\text{mol}$  and 1.3, respectively. PolyCN showed a glass transition at room temperature and a nematic-to-isotropic phase transition at  $102^\circ\text{C}$ . TetraCN showed a glass transition at  $80^\circ\text{C}$  and a nematic to isotropic phase transition at  $225^\circ\text{C}$ . TetraCN could not be crystallized from the melt. Solution-crystallized samples showed a melting temperature of  $127^\circ\text{C}$ .

The room-temperature photopolymerization of mixtures of C6Ph and CB6 or K21 was investigated using DSC. Examples of the DSC traces obtained for the polymerization are shown in Fig. 3. The enthalpy of polymerization of acrylate groups

is 78 KJ/mol.<sup>18)</sup> It can be calculated from the heat effects that with all compositions used, the conversion of the acrylate groups exceeded 50% within a few minutes of irradiation. With mixtures with higher concentrations of monoacrylate or K21 the degree of conversion exceeded 75%. These conversions are sufficiently high to stabilize the director structures of the layers. If necessary, heat treatments can be used to further increase the conversion.

The polymerization of liquid crystals between two glass plates provided with alignment layers yielded well-aligned birefringent films. Previously, it was shown that in liquid crystal mixtures containing crosslinkers, the order of the liquid crystal phase of the monomer is generally preserved during the polymerization.<sup>10,11)</sup> In the experiments described here no changes in optical properties were observed during the polymerization of the mixtures either.

The refractive indices of the polymerized layers decreased with increasing crosslinker contents. Figure 4 shows the refractive indices of the foils.

The birefringence of polymerized C6Ph was 0.095 while the birefringence of K21 was 0.19. The refractive indices of the polymerized mixtures containing CB6 were somewhat higher than the corresponding refractive indices of the mixtures containing K21. The birefringences of polyCN and tetraCN were 0.19 and 0.28, respectively.

The pretilt of the liquid crystals on the alignment layers was virtually independent of the composition of the mixture and was 2°.

### 3.2 Analysis of spincoated layers

Well-aligned liquid crystal films were obtained after spin-coating and subsequent polymerization of the liquid crystals. However, especially with thick layers (>1 μm), care had to be taken to avoid reverse tilt regions. For the experiments the thickness of the layers was kept at 0.6 μm. The retardation as a function of the angle of incidence (ϕ) can be used as a measure of the orientation of the liquid crystals. Two examples of measurements of the retardation of the samples as a function of the angle of incidence are shown in Fig. 5. For the retardation profile for the layer with a high concentration of CB6 the asymmetry with respect to the y-axis is very strong. The retardation profile for the layer prepared with a low con-

centration of CB6 the profile is much more symmetric.

Only if the average tilt angle of the liquid crystals in the layer with respect to the polyimide surface is 0° or 90° will the retardation profile be symmetric with respect to the y-axis. In the latter case the retardation at normal incidence will be zero.

Conoscopic images give a more detailed view of the director structures of the retarders. In Fig. 6 conoscopic images are presented for a retarder prepared from a mixture with a high percentage of CB6 and a retarder prepared from C6Ph. The contours are symmetric with respect to the x-axis and asymmetric with respect to the y-axis. These images indicate that the optical axes of the foils are in both cases tilted and that the foils are not twisted. In the case of the retarder prepared from a mixture containing 75%CB6 and 25%C6Ph the asymmetry is much more pronounced than in the case of the retarder prepared from 100%C6Ph.

It can be concluded from both the conoscopic and the retardation measurements that the optic axis of the foils is tilted. We used the retardation profile to determine the director profile of the liquid crystals in the layers.

The retardation ( $R$ ) as a function of tilt angle ( $\Theta$ ) in the layer is given by eqs. (1) and (2).<sup>19)</sup> For an explanation of the symbols, see Fig. 7.

$$\frac{R}{d} = \frac{n_o^2 - n_e^2}{n^2} \sin \Theta \cos \Theta \sin \Phi + \frac{n_o n_e}{n^2} \sqrt{n^2 - \sin^2 \Theta} - \sqrt{n_o^2 - \sin^2 \Theta} \quad (1)$$

$$n^2 = n_o^2 \cos^2 \Theta + n_e^2 \sin^2 \Theta \quad (2)$$

This formula could be fitted through the data points yielding the average tilt angle of the molecules in the layer. Good fits were obtained for low average tilt angles (average tilt angles < 20°). The fits became poorer for higher average tilt angles (Fig. 8). The presence of a strong tilt gradient throughout the layer is most likely the cause of the deviations.

Therefore the formula was extended to include a tilt gradient in the molecules from the polyimide surface to the liquid crystal-air interface. An indication for the tilt angle profile through the layer can be obtained from continuum mechanics.<sup>20)</sup> We will start with the situation in which the liquid crystal is strongly anchored to the polyimide layer and that

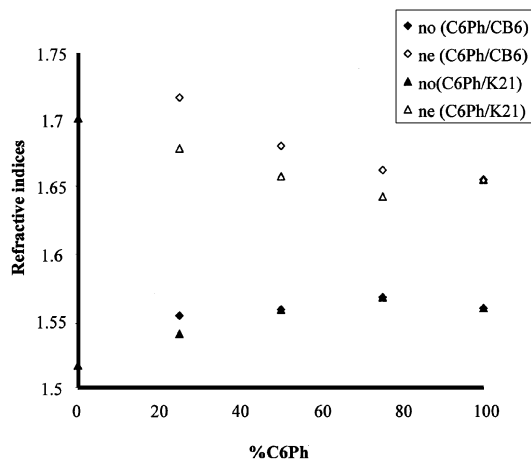


Fig. 4. Refractive indices of polymerized mixtures of C6Ph/CB6 and C6Ph/K21.

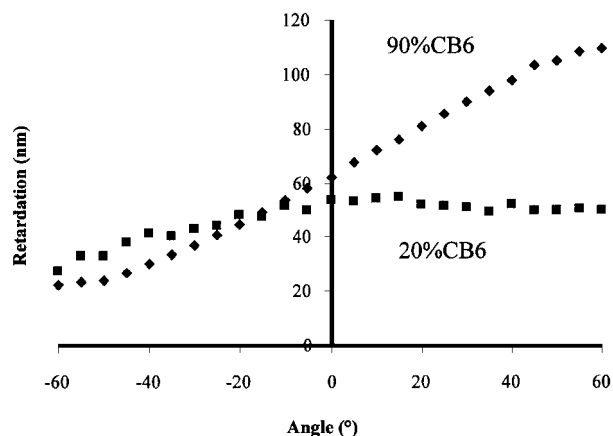


Fig. 5. Example of two retardation curves measured of samples containing different amounts of CB6 and C6Ph.

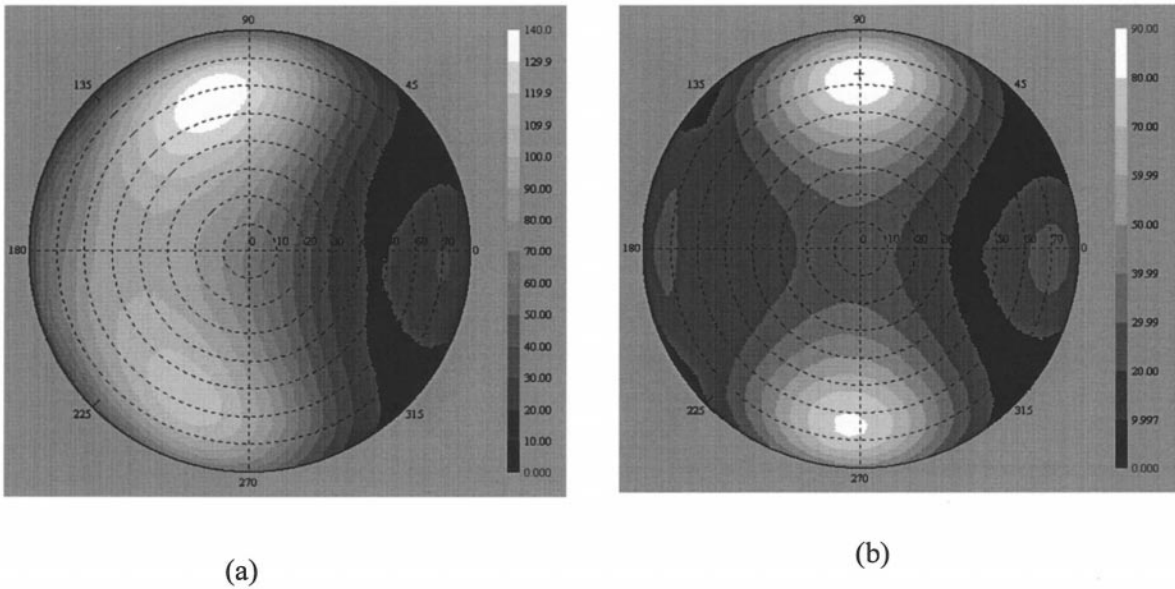


Fig. 6. Conoscopic images of retarders. (a) 75%CB6/25%C6Ph (b) 100%C6Ph.

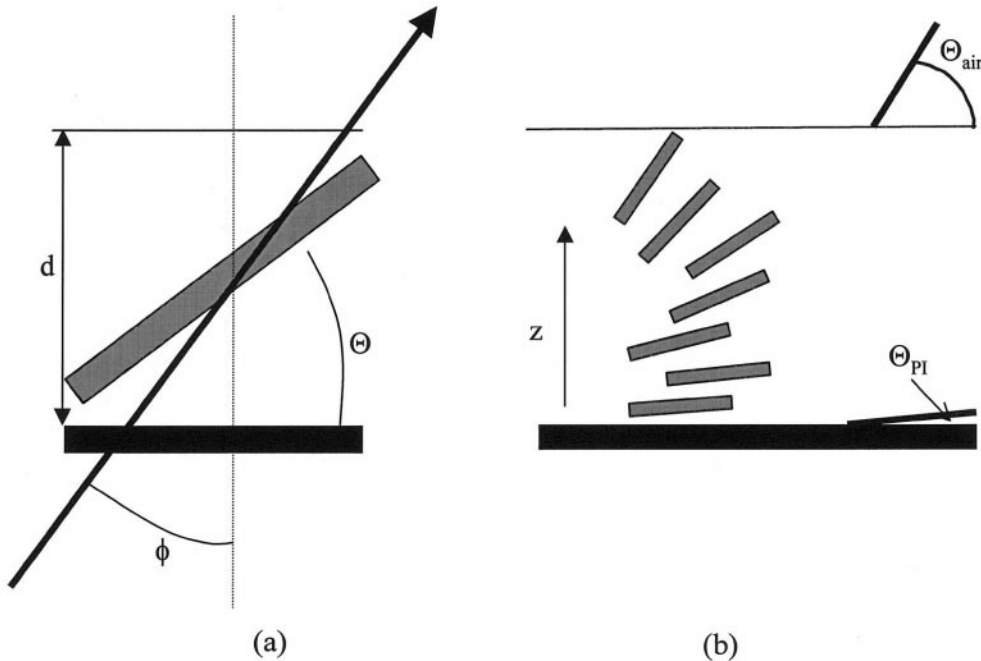


Fig. 7. Schematic representations of the director profiles in the layer. (a) Average director orientation (b) Splayed director profile.

the anchoring at the free substrate is weak with a preferential direction of the homeotropic state. There is a gradual transition from the tilt angle at the polyimide layer to the tilt angle at the air interface. The director profile in the film is governed by the following expression for the free energy:

$$F = F_s + \int_0^d dz f_b \quad (3)$$

$f_b$  and  $F_s$  are the bulk free energy density and the surface free energy, respectively.

$$f_b = \frac{1}{2} K_3 (1 - \gamma \cos^2 \Theta) (\Theta')^2 \quad (4)$$

$$F_s = \frac{1}{2} W_{\text{air}} \sin^2 \left( \Theta_{\text{air}} - \frac{\pi}{2} \right) + \frac{1}{2} W_{\text{PI}} \sin^2 \Theta_{\text{PI}} \quad (5)$$

$\Theta' = d\Theta/dz$ ,  $W_{\text{air}}$  and  $W_{\text{PI}}$  are the anchoring energy coefficients for the interfaces.  $\gamma$  is a function of the bend elastic constant  $K_3$  and the splay elastic constant  $K_1$ :

$$\gamma = \frac{K_3 - K_1}{K_3} \quad (6)$$

The Euler Lagrange equation for the director profile reads:

$$\frac{\partial f}{\partial \Theta} = \frac{d}{dz} \left[ \frac{\partial f_b}{\partial \Theta'} \right] \quad (7)$$

Substitution of the above given expressions yields:

$$K_3 \gamma \cos \Theta \sin \Theta = \frac{d}{dz} [K_3 (1 - \gamma \cos^2 \Theta) \Theta'] \quad (8)$$

The equations are more transparent if the splay and bend elastic constants are equal ( $\gamma = 0$ ). Then  $d\Theta'/dz = 0$ , so the

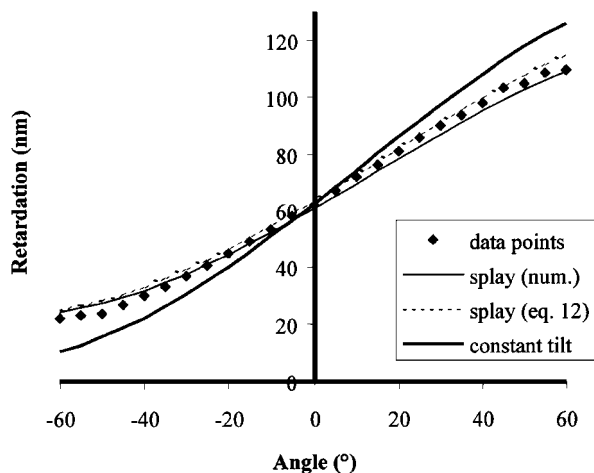


Fig. 8. Fits obtained with the average tilt approximation [Fig. 7(a)] and the splayed director profile [Fig. 7(b), numerical expressions] using the tilt angle at the liquid crystal-air interface or the average tilt angle as a fit parameter. For comparison, the curve obtained with the analytical equation (12) inserting the tilt values from the numerical procedure is shown as well.

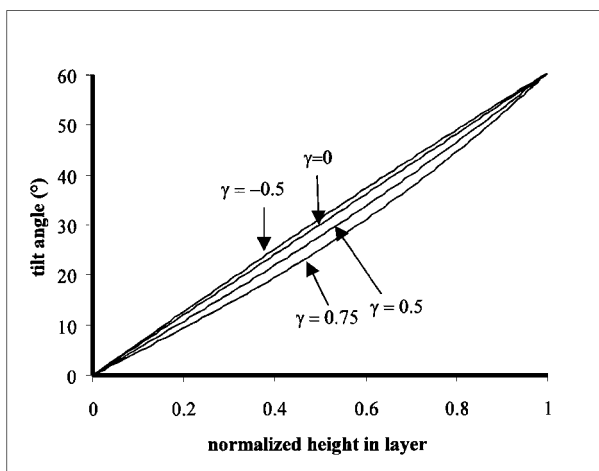


Fig. 9. Tilt angles as a function of position in the layer for varying values of  $\gamma$ . For the calculations the surface tilt was  $0^\circ$  and the tilt at the air-liquid crystal interface was  $60^\circ$ .

tilt varies linearly with the position.

$$\Theta(z) = (\Theta_{\text{air}} - \Theta_{\text{PI}}) \frac{z}{d} + \Theta_{\text{PI}} \quad (9)$$

A more detailed calculation shows that within the usual variation of the splay and bend elastic constants ( $\gamma \neq 0$ ) the deviations from the linearity are small. For an example, see Fig. 9.

The tilt at the free surface is determined by the layer thickness, the anchoring energy coefficients for both surfaces, the elasticity of the liquid crystal, and the tilt at the polyimide substrate. In the case that  $\gamma = 0$  ( $K_3 = K_1 \equiv K$ ), we find that:

$$\Theta_{\text{air}} - \Theta_{\text{PI}} = \frac{W_{\text{air}} d}{2K} \sin 2\Theta_{\text{air}} = \frac{W_{\text{PI}} d}{2K} \sin 2\Theta_{\text{PI}} \quad (10)$$

If  $W_{\text{PI}} \gg W_{\text{air}}$  than  $\Theta_{\text{PI}} \approx 0$  and

$$\Theta_{\text{air}} - \frac{W_{\text{air}} d}{K} \sin \Theta_{\text{air}} \cos \Theta_{\text{air}} = 0 \quad (11)$$

This equations shows that there exists a certain minimum layer thickness above which a finite tilt angle can exist:<sup>21)</sup>

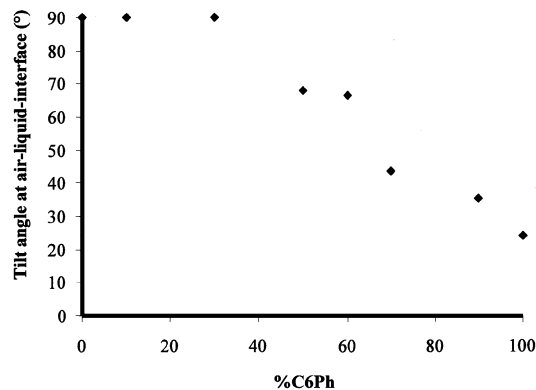


Fig. 10. Tilt angle at air-liquid interface for C6Ph/K21 mixtures.

If  $d \leq K/W_{\text{air}}$  then  $\Theta_{\text{air}} = 0$ ,  $d > K/W_{\text{air}}$  then  $\Theta_{\text{air}} \neq 0$ .

Using eqs. (9) and (1) the retardation profiles can be analyzed. It is possible to obtain a closed expression for the retardation of layers with a tilt gradient by assuming that  $\Delta n \ll 1$ .

$$R = \frac{d\Delta n}{\cos \alpha} \left[ \frac{1}{2} + \frac{1}{4} \frac{\sin(2\Theta_{\text{air}} - 2\alpha) - \sin(2\Theta_{\text{PI}} - 2\alpha)}{\Theta_{\text{air}} - \Theta_{\text{PI}}} \right] \quad (12)$$

$$\alpha = \arcsin \left( \frac{\sin \phi}{n_o} \right) \quad (13)$$

For our experiments the retardation as a function of the viewing angle of splayed director profiles was analyzed by dividing the layer into 50 sublayers with constant tilt and adding up the retardations of the sublayers using eqs. (1) and (9). The experimental data could be fitted very well using the measured thickness (see example in Fig. 8, thickness:  $0.6 \mu\text{m}$ , tilt angle at liquid crystal-air interface:  $80^\circ$ ). In Fig. 8 also the retardation values calculated with eq. (12) using the parameters obtained from the fit procedure are shown. The agreement with the numerically calculated values is satisfactory.

The tilt angles at the liquid crystal-air interface were calculated from the retardation profiles using the numerical procedure. In Fig. 10 the calculated tilt angle at the liquid crystal-air interface is shown as a function of composition of polymerized mixtures of C6Ph and K21. It is clear that the orientation at the interface is homeotropic in the case of liquid crystals containing large amounts of K21. The tilt angle gradually decreases with increasing amounts of C6Ph. The value for 100% C6Ph is approximately  $24^\circ$ . In the case of CB6 the behaviour of the mixtures is similar (Fig. 11). At high CB6 contents the orientations at the liquid crystal-air interface are close to homeotropic, while the values are low at high cross linker contents.

Well-aligned layers of polyCN and tetraCN could be obtained by heating the spincoated layers to temperatures between the glass transition temperature and the nematic-to isotropic-transition. The higher the temperature, the faster the alignment of the liquid crystals. Good alignment was usually obtained within a few minutes of equilibration. Examples of retardation profiles for the glass-forming compounds are shown in Fig. 12. The retardation profiles are more or less symmetrical around the  $y$ -axis. The tilt angles calculated for both compounds correspond to the pretilt angle generated by the polyimide alignment layer. The low tilt angles were also found in layers with a thickness of several microns.

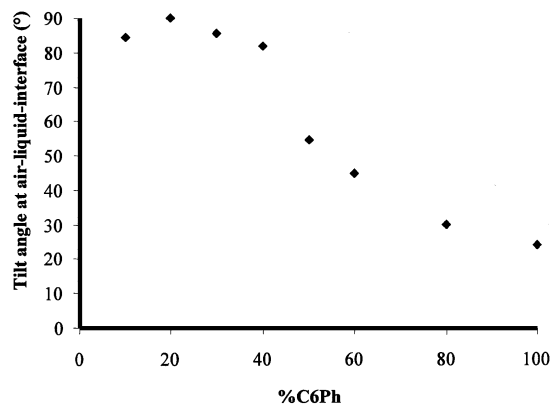


Fig. 11. Tilt angle at air-liquid interface for mixtures containing C6Ph and CB6.

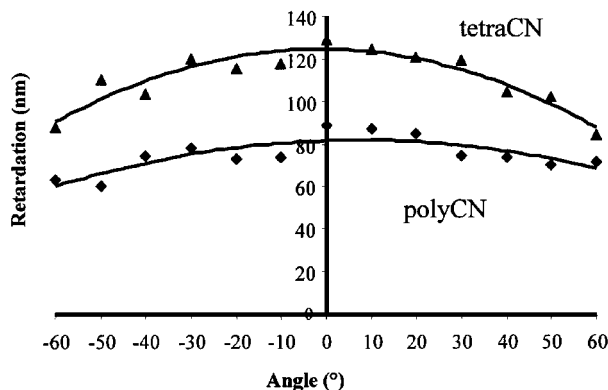


Fig. 12. Retardation profiles of layers containing tetraCN and polyCN.

#### 4. Discussion

It has been demonstrated that a large variety in tilt angles can be produced by varying the composition of the liquid crystal mixture. Very low tilt angles were obtained by processing polyCN and tetraCN. High tilt angles could be obtained using mixtures of reactive liquid crystals. The tilt angles were preserved during photopolymerization of the reactive liquid crystals.

In the case of reactive liquid crystal mixtures containing large fractions of K21 or CB6 the liquid crystals tend to align homeotropically at the liquid crystal-air interface. The tilt angles decrease strongly with increasing fractions of diacrylate. The high tilt angles of the mixtures containing large fractions of K21 or CB6 can be attributed to the mixed polarity of these molecules. For energetic reasons the polar cyano head of the molecule tends to point away from the air-liquid crystal interface and the apolar alkyl end group tends to point to the air-liquid crystal interface. This leads to a strong preference for homeotropic orientation. Hikmet *et al.* used the same principle for the preparation of pretilt amplification layers: when a thin layer of a mixture of LC diacrylate and a commercial cyanobiphenyl mixture was polymerized on a polyimide alignment layer, the pretilt angles of liquid crystals at the polymerized liquid crystal surface were higher than at the polyimide surface.<sup>22)</sup> Interfaces are known to induce additional ordering in nematic liquid crystalline phases often leading to the formation of smectic layers at the liquid crystal-

air interface.<sup>23–25)</sup> It is well-known that cyanobiphenyls have a tendency to pack in antiparallel dipole associations.<sup>26,27)</sup> Similar associations between CB6 residues were found by Hikmet *et al.* in polymerized mixtures of CB6 and a liquid crystalline diacrylate with a structure similar to that of C6Ph (C6M).<sup>12)</sup> Such smectic surface layers may form an additional stabilizing factor for homeotropic orientation at the interface.

In the case of the polymeric liquid crystal polyCN the tilt angle of the molecules resulting in the layer was close to zero. Due to the large difference in polarity between the backbone and the side chain, polyCN can also be expected to have a preference for homeotropic orientation of the molecules at the interface. Large differences in the elastic constants could be a possible reason for deviations [see eq. (11)]. However, published data on the values of elastic constants of liquid crystalline side chain oligomers indicate that these values are similar to those of low molecular weight liquid crystals.<sup>28–30)</sup> Jérôme and colleagues suggested that steric reasons may be responsible for the preference for planar orientation of liquid crystalline polymers with polar side chains.<sup>31)</sup> For a homeotropic orientation the apolar backbone is energetically favoured at the liquid crystal-air interface, the side chains point into the liquid crystal layer. Due to the steric requirements relating to the spacing of the side chains there is insufficient space for all the side chains to point away from the surface and to pack in the antiparallel dipole associations.

The tilt angle of layers of tetraCN was also close to zero. Most likely this low tilt angle is related to the symmetric chemical structure of the molecule. All four arms of the molecule are substituted with the polar cyano-biphenyl group. Due to the lack of energetic preferences for a homeotropic orientation of the molecules at the interface, the planar orientation of the molecules at the polyimide alignment layer can be maintained throughout the layer.

Future work on materials containing these and other mesogenic groups is required to further elucidate the complex relations between surface tilt and molecular structure.

#### 5. Conclusions

Mixtures of CB6 or K21 and C6Ph can be used to prepare layers with high average tilt angles for the optic axis. Mixtures with high concentrations of CB6 or K21 align planarly at the polyimide liquid crystal interface and tend to align homeotropically at the liquid crystal-air interface. The value of the tilt angle can be controlled by tuning the mixture's composition. The symmetrically substituted tetraCN can be used to prepare layers with a low tilt angle. Despite the presence of polar and apolar moieties in the molecule, also polyCN also yields very low tilt angles. Most likely steric reasons are responsible for the differences obtained for low molecular weight and polymeric substances.

#### Acknowledgements

We thank Rifat Hikmet and Dick Broer for helpful discussions, and Jack van den Eerenbeemd for his help with the analysis of the retardation profiles.

1) S.-T. Wu: *Mat. Chem. Phys.* **42** (1995) 163.

2) Y. Fujimura, T. Nagatsuka, H. Yoshimi, S. Umemoto and T. Shimomura: *SID Dig.* (1992) 397.

- 3) Y. Fujimura, T. Nagatsuka, H. Yoshimi and T. Shimomura: SID Dig. (1991) 739.
- 4) I. Heynderickx and D. J. Broer: Mol. Cryst. & Liq. Cryst. **203** (1991) 113.
- 5) M. Bosma, P. P. de Wit, A. Steenbergen and S. J. Picken: SID Dig. (1997) 679.
- 6) J. Mukai, T. Kurita, T. Kaminade, H. Hara and T. Toyooka, H. Itoh: SID Dig. (1994) 241.
- 7) H. Mori, Y. Itoh, T. Nishiura, T. Nakamura and Y. Shinagata: Jpn. J. Appl. Phys. **36** (1997) 143.
- 8) P. van de Witte, S. Stallinga and J. A. M. M. van Haaren: SID Dig. (1997) 687.
- 9) P. van de Witte, S. Stallinga and J. A. M. M. van Haaren: IDW Dig. (1997) 395.
- 10) D. J. Broer: *Liquid Crystals in Complex Geometries*, eds. G. P. Crawford and S. Zumer (Taylor and Francis, London, 1996) p. 239.
- 11) R. A. M. Hikmet and J. Lub: Prog. Polym. Sci. **21** (1996) 1165.
- 12) R. A. M. Hikmet, J. Lub and P. Maassen van den Brink: Macromolecules **25** (1992) 4194.
- 13) D. J. Broer, J. Boven, G. N. Mol and G. Challa: Makromol. Chem. **190** (1989) 2255.
- 14) P. van de Witte, J. C. Galan and J. Lub: Liq. Cryst. **24** (1998) 819.
- 15) J. Lub and P. van de Witte, to be published in Liq. Cryst.
- 16) H. A. van Sprang: Mol. Cryst. Liq. Cryst. **199** (1991) 19.
- 17) S. Stallinga, J. M. A. van den Eerenbeemd and J. A. M. M. van Haaren: Jpn. J. Appl. Phys. **37** (1998) 560.
- 18) *Polymer Handbook*, eds. J. Brandrup and E. H. Immergut (John Wiley & Sons, New York, 1975) 2nd ed.
- 19) M. Françon: *Handbuch der Physik XXIV: Grundlagen der Optik*, ed. S. Flügge (Springer-Verlag, Berlin, 1956) p. 439.
- 20) G. Vertogen and W. H. de Jeu: *Thermotropic Liquid Crystals: Fundamentals* (Springer-Verlag, Berlin, 1988) Chaps. 5 and 6.
- 21) G. Barbero and R. Barberi: J. Phys. (Paris) **44** (1983) 609.
- 22) R. A. M. Hikmet and C. de Witz: J. Appl. Phys. **70** (1991) 1265.
- 23) P. S. Pershan: J. Phys. (Paris) **7** (1989) 1-20.
- 24) B. Jérôme: Rep. Prog. Phys. **54** (1991) 391.
- 25) E. F. Gramsbergen, W. H. de Jeu and J. Als-Nielsen: J. Phys. (Paris) **47** (1986) 711.
- 26) A. J. Leadbetter, J. C. Frost, J. P. Gaughan, G. W. Gray and A. Mosley: J. Phys. (Paris) **40** (1979) 375.
- 27) A. J. Leadbetter and A. I. Mehta: Mol. Cryst. Liq. Cryst. **72** (1981) 51.
- 28) E. E. Pashkovsky, T. G. Litvina, S. G. Kostromin and V. P. Shibaev: J. Phys. II (Paris) **2** (1992) 1577.
- 29) H. J. Coles and M. S. Bancroft: Mol. Cryst. Liq. Cryst. **237** (1993) 97.
- 30) V. P. Shibaev, S. G. Kostromin and S. A. Ivanov: *Polymers as Electro-optical and Photo-optical Active Media*, ed. V. P. Shibaev (Springer-Verlag, Berlin, 1996) p. 37.
- 31) B. Jérôme, J. Commandeur and W. H. de Jeu: Liq. Cryst. **22** (1997) 685.